Mid-infrared difference-frequency generation of ultrashort pulses tunable between 3.2 and 4.8 μm from a compact fiber source

C. Erny, K. Moutzouris, and J. Biegert

ETH Zurich, Physics Department, Institute of Quantum Electronics, Wolfgang-Pauli Strasse 16,
8093 Zürich, Switzerland

D. Kühlke

Furtwangen University of Applied Sciences, Department of Computer & Electrical Engineering, Robert-Gerwig-Platz 1,
78120 Furtwangen, Germany

F. Adler and A. Leitenstorfer

Department of Physics and Center for Applied Photonics, University of Konstanz, Universitätsstr. 10,
78457 Konstanz, Germany

U. Keller

ETH Zurich, Physics Department, Institute of Quantum Electronics, Wolfgang-Pauli Strasse 16,
8093 Zürich, Switzerland

We report single-pass difference-frequency generation of mid-infrared femtosecond pulses tunable in the 3.2–4.8 μm range from a two-branch mode-locked erbium-doped fiber source. Average power levels of up to 1.1 mW at a repetition rate of 82 MHz are obtained in the mid infrared. This is achieved via nonlinear mixing of 170 mW, 65 fs pump pulses at a fixed wavelength of 1.58 μm, with 11.5 mW, 40 fs pulses tunable in the near-infrared range between 1.05 and 1.18 μm. These values indicate that the tunable near-infrared input component is downconverted with a quantum efficiency that exceeds 30%. © 2007 Optical Society of America

OCIS codes: 190.2620, 140.3510, 140.3580, 140.4050.

Sources of tunable mid-infrared (mid-IR) ultrashort pulses are of great interest for use in various applications, ranging from vibrational spectroscopy via trace-gas detection to high-field science. Because suitable laser gain media are limited for this wavelength range, downconversion of near-infrared (near-IR) sources by difference-frequency generation (DFG), optical parametric generation (OPG), or optical parametric oscillation (OPO) remains the most common approach for accessing the mid-IR.[1] DFG offers straightforward single-pass geometries relative to OPO and offers higher conversion efficiencies compared with OPG. In addition, difference-frequency mixing of two input pulses with random phase but equal phase fluctuations in the electric field oscillation results in the production of a carrier-envelope-offset (CEO) phase-stabilized output[2,3] without the need for active stabilization. Our interest is to use this compact source as a CEO phase-preserving seed for chirped-pulse optical parametric amplifiers[4,5] (CPOPAs) and single attosecond pulse generation, because the mid-IR wavelength substantially extends the cut-off energy in high harmonic generation.[6]

So far a mode-locked Ti:sapphire laser has typically been used for femtosecond nonlinear mid-IR generation. This laser is relatively complex and expensive. More recently compact femtosecond fiber lasers have offered an attractive alternative to the Ti:sapphire oscillator, and additional upconversion schemes have extended their spectral coverage from ultraviolet to the visible and near infrared.[7,8]

In this Letter we describe a single-pass difference-frequency mixer for the mid-IR comprising a two-branch mode-locked Er:fiber pump source and a $MgO:LiNbO_3$ crystal as the nonlinear medium. It delivers femtosecond pulses with an average power of up to 1.07 mW of mid-IR radiation tunable in the wavelength range between 3.2 and 4.8 μm at a repetition rate of 82 MHz. Both negligible phase drifts between the two pump-laser branches[9] and negligible phase noise of the continuum generation[10] have been demonstrated and indicate that the generated mid-IR radiation should be phase stabilized. The specifications of the present source are ideal for various applications, including CPOPAs and frequency-comb Fourier-transform infrared spectroscopy.[11]

The experimental setup is schematically illustrated in Fig. 1. The pump-source configuration has been described in detail.[12] The mode-locked fiber oscillator seeds two separate amplifier stages, each delivering 65 fs pulses centered at a wavelength of 1.58 μm with an average power of 250 mW and a repetition rate of 82 MHz. The output of the second amplifier is coupled into a highly nonlinear fiber[12] (HNLF) with the zero-dispersion wavelength around 1.52 μm and a core diameter of 3.7 μm. The HNLF output comprises near-IR pulses that are tunable in
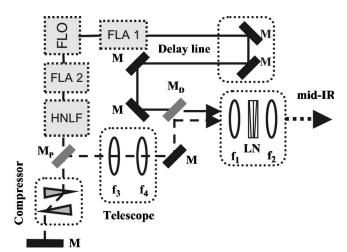
Fig. 1.   Experimental setup: M, gold-coated mirrors; FLO, fiber-laser oscillator; FLA, fiber-laser amplifier; HNLF, highly nonlinear fiber; f_i, lenses of focal length of 30, 40, −30, and 75 mm, for $i = 1$, 2, 3, and 4, respectively; LN, fan-out poled $MgO:LiNbO_3$ nonlinear crystal. The solid line indicates the beam path of the fundamental laser component at 1.58 μm. The dashed line follows the tunable near-IR component.

the 1.05–1.4 μm wavelength range with an average power of more than 20 mW. From the entire tuning range of the HNLF output we utilize only the 1.05–1.18 μm wavelength band in the present experiment. This near-IR component is compressed with a prism pair to sub-40 fs and then passed through a two-lens telescopic arrangement that allows control of the beam waist. The fundamental radiation from the first amplifier (1.58 μm, 65 fs, 250 mW) is temporally and spatially overlapped with the tunable near-IR component of the second branch (1.05 μm−1.18 μm, <40 fs, 20 mW, $\Delta\tau\Delta\nu=0.33$) using a delay line and a proper dichroic mirror, respectively. A single input lens focuses the two copropagating beams to a measured $1/e^2$ beam diameter of 22 μm, into the center of a 2 mm thick quasi-phase-matched $MgO:LiNbO_3$ crystal. The nonlinear crystal has a continuously variable grating period Λ ranging from $\Lambda=21$–34 μm. This fan-out design permits continuous tuning of the mid-IR output from 3 μm up to the absorption cutoff wavelength of the nonlinear medium (approximately 5 μm) by simple linear translation of the sample. The $MgO:LiNbO_3$ crystal is antireflection (AR) coated at all wavelengths of interest at both facets and heated to approximately 80°C to avoid photorefractive damage. The output radiation is collimated with an additional uncoated CaF_2 lens and transmitted through a 1 mm thick germanium filter to ensure that only the mid-IR pulses are collected.

After alignment optimization, the mid-IR radiation can be measured directly on a thermal powermeter. Figure 2 illustrates a selection of typical normalized mid-IR spectra, measured with a grating monochromator and a cooled HgCdTe (MCT) detector together with a lock-in amplifier. They demonstrate an overall tuning range extending from 3.2 up to 4.8 μm. The tuning range of our device is limited only by absorp-

tion in $MgO:LiNbO_3$ and could be extended to longer wavelengths (up to 12 μm) with other nonlinear crystals (e.g., GaSe). A sudden dip appearing near 4.2 μm is due to carbon dioxide absorption. Typical FWHM spectral bandwidths of 200 to more than 300 nm are obtained throughout the mid-IR.

Figure 3 presents measurements of the mid-IR average power versus central wavelength. Up to 1.07 mW is generated around 3.6 μm for pump power levels (measured before the input facet of the nonlinear crystal) that do not exceed 11.5 mW in the near-IR and 170 mW at 1.58 μm. These values indicate that the near-IR beam is downconverted with a quantum efficiency (defined as $N_{mid-IR}/N_{near-IR}$, where N is the number of photons at the respective wavelength) of more than 30%. Average power at the "blue" end of the tuning range is mainly reduced due to the lower power of the corresponding near-IR component, which is close to the cutoff wavelength of the HNLF (1.05 μm). On the other side, the mid-IR power at the "red" wing of the tuning range is reduced due to increased crystal absorption and an accepted compromise in the performance of the present crystal AR coating. It is to be noted that at least 0.5 mW of mid-IR radiation is obtained at wavelengths between 3.3 and 4.0 μm. The generated output power was also measured as a function of the average power of the two input components. It was found that the mid-IR radiation increases linearly with increasing power in the tunable near-IR. However, saturation of gain is observed for input power levels at 1.58 μm exceeding approximately 80 mW. Therefore power scaling of the present source should primarily address optimization of the HNLF output.

Due to the modest available power levels, direct autocorrelation measurements of the output pulse duration were not possible with the available instruments. For a theoretical simulation of the nonlinear evolution process, we employed a fully three-dimensional wave propagation model.[13] Full temporal, spectral, and phase information for both input pulses in the model were measured with a frequency-resolved-optical-gating[14] (FROG) technique. We then measured (Fig. 4, squares) and calculated (Fig. 4, solid curve) the normalized DFG signal at a center wavelength of 3.6 μm as a function of the
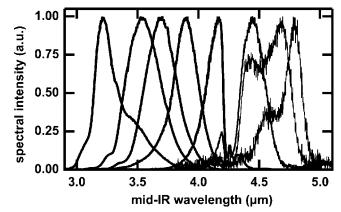

Fig. 2.   Typical selection of normalized mid-IR spectra throughout the tuning range of the DFG converter.
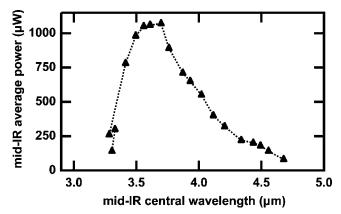
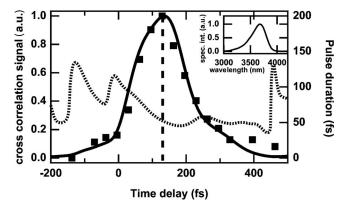Fig. 3. Mid-IR average power as a function of central wavelength.

Fig. 4. Theoretical three-dimensional DFG power (solid curve) and pulse duration (dotted curve) as a function of near-IR input pulse delay. Comparison with experimental measurements (squares) exhibits excellent agreement. The simulated spectrum at a central wavelength of 3.6 μm (inset) results in 330 nm FWHM. This value also agrees with experimental measurements (see the experimental spectra in Fig. 2). Maximum output power occurs for a time delay of 130 fs, corresponding to a theoretical pulse duration of 53 fs. Positive time delay values assume a leading 1.58 μm pulse.

temporal delay between the two near-IR input pulses directly after the nonlinear crystal. In addition, theory predicted a spectral width of 330 nm (inset in Fig. 4), which agrees well with the experimental result of 300 nm. These agreements confirm the validity of the theoretical model. Maximum output power is calculated for a 130 fs input delay, corresponding to a theoretical pulse duration of 53 fs. The 53 fs pulses with 300 nm spectral bandwidth (both at a center wavelength of 3.6 μm), leads to a time–bandwidth product of $\Delta\nu\Delta\tau\approx 0.37$.

Finally, we established that the generated mid-IR pulses can be easily stretched to several picoseconds by simple dispersive pulse propagation. Exploiting the output of a Nd:YVO$_4$ laser-amplifier (Duetto, Time-Bandwidth Products) as reference signal in a cross-correlation setup, we measured ~5 ps pulses in

the mid IR after transmission through a 10 cm long sapphire window. This observation reveals the potential of our source for implementation in a subsequent CPOPA system.

In conclusion, we have demonstrated DFG of spectrally broad mid-IR pulses from a compact, two-branch mode-locked fiber laser. Our present setup exhibits an overall tuning range between 3.2 and 4.8 μm. Average power levels of up to 1.07 mW are measured at central wavelengths of 3.6 μm, corresponding to a maximum quantum conversion efficiency of more than 30% with respect to the near-IR pump component. Theoretical estimates, supported by experimental measurements, indicate that the generated pulses exhibit sub-100 fs durations. Previous experimental demonstration of negligible phase drift between the two amplifier branches of the fiber laser indicates that the generated mid-IR radiation should be phase stable. The specifications of our source are attractive for numerous applications, including the design of novel optical parametric amplifiers and Fourier-transform infrared spectrometers.

References

1. V. Petrov, F. Rotermund, and F. Noak, J. Opt. A, Pure Appl. Opt. **3**, R1 (2001).
2. H. R. Telle, G. Steinmeyer, A. E. Dunlop, J. Stenger, D. H. Sutter, and U. Keller, Appl. Phys. B **69**, 327 (1999).
3. Y. Deng, F. Lu, and W. H. Knox, Opt. Express **13**, 4589 (2005).
4. A. Dubietis, G. Jonusauskas, and A. Piskarskas, Opt. Commun. **88**, 437 (1992).
5. C. P. Hauri, P. Schlup, G. Arisholm, J. Biegert, and U. Keller, Opt. Lett. **29**, 1369 (2004).
6. J. L. Krause, K. J. Schafer, and K. C. Kullander, Phys. Rev. Lett. **68**, 3535 (1992).
7. K. Moutzouris, F. Adler, F. Sotier, D. Trautlein, and A. Leitenstorfer, Opt. Lett. **31**, 1148 (2006).
8. K. Moutzouris, F. Sotier, F. Adler, and A. Leitenstorfer, Opt. Express **14**, 1905 (2006).
9. F. Adler, K. Moutzouris, A. Leitenstorfer, H. Schnatz, B. Lipphardt, G. Grosche, and F. Tauser, Opt. Express **12**, 5872 (2004).
10. E. Benkler, H. R. Telle, A. Zach, and F. Tauser, Opt. Express **13**, 5662 (2005).
11. C. G. F. Keilmann and R. Holzwarth, Opt. Lett. **29**, 1542 (2004).
12. F. Tauser, F. Adler, and A. Leitenstorfer, Opt. Lett. **29**, 516 (2004).
13. G. Arisholm, Opt. Express **14**, 2543 (1997).
14. R. Trebino and D. J. Kane, J. Opt. Soc. Am. A **10**, 1101 (1993).